Journal of Thermal Analysis, Vol. 53 (1998) 717-735

A NOVEL THERMO-OPTICAL MEASURING SYSTEM FOR THE IN SITU STUDY OF SINTERING PROCESSES

*F. Raether, R. Hofmann, G. Müller and H. J. Sölter**

Fraunhofer-Institut für Silicatforschung (ISC), Würzburg
*Compotherm, Syke, Germany

(Received August 18, 1997, in revised form June 12, 1998)

Abstract

A novel thermo-optical measuring system (TOM) is described, which is able to monitor simultaneously and in situ thermal and optical properties of materials during the process of sintering. These are thermal diffusivity, heat capacity, thermal conductivity, transfer of heat radiation and scattering of light. Additionally, the geometric shrinkage is recorded by a non-contact optical dilatometer. The system has been designed for an efficient optimization of time-temperature-atmosphere cycles in sintering processes. Therefore, in the construction of the TOM system transferability of process parameters to other sintering furnaces is an important requirement. Due to this, compromises have been necessary in the layout of the measuring methods. Nevertheless, a high resolution was achieved for the distinction of different sintering states. Besides dilatometry, thermal diffusivity measurement by a laser-flash technique is a promising tool for the in situ monitoring of changes in microstructure during sintering.

Keywords: ceramics, in situ measurements, sintering, thermal analysis

Introduction

Sintering has reached a very comprehensive technological importance. Most of the powder metallurgical, ceramic and many glass ceramic components are sintered nowadays. Classical applications of sintering processes are in the production of building materials, sanitary ceramics and dishes as well as in iron powder metallurgy. Furthermore, sintered high performance materials are used in numerous key technologies, e.g. in electronics as functional or substrate material, in the tools industry as a component of cutting tools or in the production of high performance turbines as materials with high strength at high temperatures. These applications demand very specific characteristics of the sintering material, for example an especially high strength or special electrical, thermal and optical properties. Subsequent to powder production the sintering process contributes essentially to the control of these properties and, consequently, to the quality of the sintered materials [1]. The empirical optimization of sintering processes through trial and error is still a common procedure nowadays, however, very

1418–2874/98/ $ 5.00

Akadémiai Kiadó, Budapest
Kluwer Academic Publishers, Dordrecht

time-consuming. A sintering cycle has to be performed completely for several times and only after an also time-consuming analysis of the sintered samples the usefulness of the cycle may be judged.

In situ measuring methods can improve this situation. They allow to control the material properties during the very process of sintering. The most important measuring method for the in situ investigation of sintering processes is dilatometry, which detects the geometric shrinkage of the sample during sintering. Usually push rod dilatometers are used, which push one end of a rod on the sample surface and allow a very sensitive measurement of the length change at the opposite end of the rod that is outside the furnace [2]. In some cases, dilatometry has been successfully used in rate-controlled sintering (RCS) to control sintering processes through the shrinkage rate [3]. As one result of RCS, complicated time-temperature cycles for the sintering process may arise, which may differ substantially from the common cycles with constant temperatures but may lead to improved material characteristics.

The goal of the development, which is presented in this paper, is an improvement of sintering processes by constructing a measuring device, that can detect important material properties during sintering. By the in situ measurement of those properties a specific optimization of time-temperature-atmosphere cycles will become possible. Afterwards, the optimized process parameters shall be transferred to industrial sintering processes. Due to the transferability of the results, the design of the new device has to fulfil a number of requirements. First, material properties have to be detected, that are representative of the sample. Therefore, the measuring volume has to be sufficient and the sample size has to be large enough to suppress surface effects. The in situ measurements must not disturb sintering. Therefore, non-contact measurements are preferred. The measurements should be done with samples prepared similarly to the real components. For that reason special pre-treatments like coatings, that can influence sintering, are not allowed. To transfer the results to other furnaces later on, a controlled and homogeneous temperature is needed. Variable temperature schedules have to be realized and different sintering atmospheres should be feasible to achieve a broad range of applications. A complete characterization of a sample in one sintering run by measuring as many important material properties as possible is very desirable, since the use of different samples and furnaces deteriorates the comparability of the single results.

The basic information in sintering processes comes from the shrinkage measurement. Therefore, dilatometry has to be integrated in the design of the new device. Besides dilatometry the in situ measurement of thermal, optical and mechanical properties seems to be promising. Due to improvement of sensor techniques, non-contact detection of the measuring signals is possible for all three fields. Various types of lasers are available for the excitation of the measuring signals. For the non-contact measurement of mechanical properties, ultrasound waves can be produced in the sample by rapid heating of the sample surface with

a short laser pulse. The speed of the ultrasound waves can be measured by interferometric observation of the sample surface. From the speed of ultrasound waves the elastic modulus of the samples is determined [4]. By irradiating the sample surface with a modulated laser beam, vibrations of the sample can be excited. The amplitude of the vibrations can be measured by interferometric methods, too. From the Eigen frequency the elastic modulus can be calculated. The width of the resonance peak depends on the adhesion of particles in a powder compact [5]. A pulse technique for the measurement of thermal diffusivity was already developed in the early seventies [6]. The front side of a disk shaped sample was heated by the short pulse of a Xenon lamp and the temperature rise at the rear side was measured by a thermocouple. The technique was improved by generating the short light flash by a pulsed laser (laser flash technique). Later on by measuring the temperature with fast and sensitive pyrometers, non-contact measurement of thermal diffusivity was achieved [7–10]. Besides the laser-flash technique, thermal diffusivity can be determined by the Ångstrom method, where a modulated laser beam is used to generate thermal waves in the sample [11]. The phase shift between the exciting laser beam and the surface temperature of the sample depends on the thermal diffusivity of the sample and can be recorded non-contact by pyrometers, as well [12]. A comparison between the two measurement methods is given in [13]. Thermal material properties like thermal diffusivity or thermal conductivity are a promising tool to monitor microstructural phenomena during sintering, since a strong dependence of these properties on microstructural changes is expected. By using continuous or modulated laser beams light scattering properties of a sample can be detected in situ by measuring the attenuation of the laser beam in the sample or by measuring the intensity of the scattered light. To achieve a sufficient measuring volume, wavelengths are used, where the sample has a low absorption [14]. Optical properties can also give insight in the microstructure of sintering materials. In the final stage of sintering light scattering is strongly influenced by the presence of a small fraction of pores [15]. Since the detection of a small pore fraction is difficult by other methods, light scattering should be a useful tool for the study of the final stage of sintering [16]. In the following, mainly the simultaneous determination of sintering shrinkage and thermal diffusivity will be presented. The in situ measurement of optical material properties will be reported in more detail in a separate paper.

Experimental set-up

A new thermo-optical measuring system (TOM) was constructed for the simultaneous in-situ measurement of thermal and optical material properties and sintering shrinkage. Figure 1 shows the layout of the TOM-system and Fig. 2 represents a sketch of the furnace type used with the system. Many of the requirements described in the previous section refer to the furnace which, therefore had

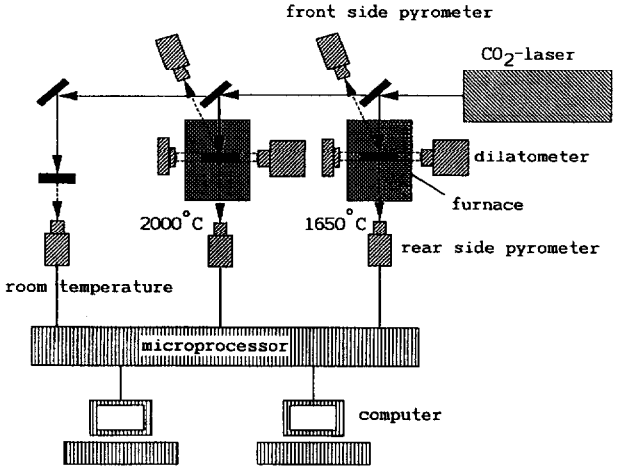

Fig. 1 Sketch of the thermo-optical measuring system (TOM) with three measuring sites for room temperature measurements and measurements up to 2000 and 1650°C respectively

to be especially designed. The cylindrical axis of the furnace is in the vertical direction. The combustion chamber which is located in the centre of the furnace has a diameter of 10 cm and a height of 12 cm. A ring shaped sample holder is positioned in the centre of the furnace which has a sharp edge at its upper side to minimize interaction with the sample. The thermal insulation is about 8 cm thick and contains only small windows with a diameter of 2 cm for the excitation and detection of the measuring signals. Two opposing windows lie in the horizontal direction and two other windows lie along the vertical axis of the furnace. The rest of the windows is arranged with an angle of 15° from the centre of the combustion chamber to the vertical axis (Fig. 2). From the centre of the chamber the aperture angle from the sample to the windows at the top and the bottom of the furnace is about 6°. The furnace is enclosed in a water-cooled vacuum-tight housing of high grade steel. Each of the through holes leads to a window made of quartz glass in the horizontal direction and of NaCl and ZnSe in the other directions, respectively. NaCl and ZnSe are used because of their good transmission in the long IR-range. (Some of the windows are reserved for additional measurements of optical material properties and are not used in the experiments described in the present paper.) Shutters that are only shortly opened in intervals during the measurements protect the windows against condensation of volatile components of the sample. Additionally, gas inlets near the windows direct the furnace gas inward and therefore reduce the gas flow from the sample to the windows. Gas flow is controlled by an electronic flow meter. It can be varied between 0.002 and 2 l min^{-1}. Two different gases can be mixed and the mixing ratio can be varied by computer control in the range of 0.2 to 99.8 vol% [17]. A pneu-

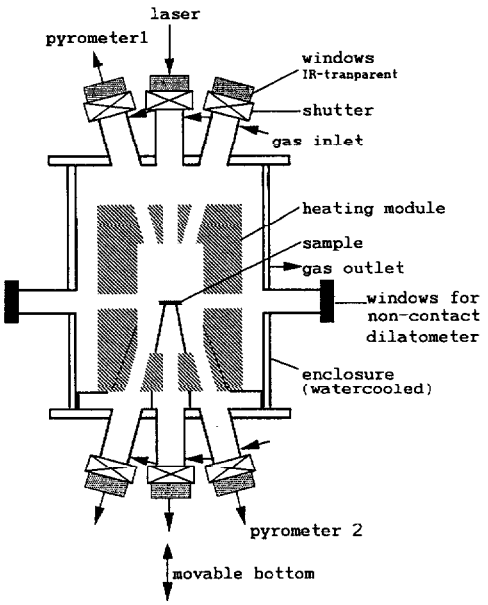

Fig. 2 Construction of the furnaces used with the TOM system

matic drive can move the bottom part of the furnace together with the sample holder downward and upward. In the open position of the furnace a gripping device can automatically exchange the sample. The gripping device uses negative pressure for the careful manipulation of the sample [18]. Direct current and a special current control are used for the electrical heating of the furnaces thus minimizing electromagnetic noise, which could disturb the measurements. To realize reducing as well as oxidizing furnace atmospheres at high temperatures, two furnaces had to be built. One of them uses graphite heating elements, an insulation of graphite fibres and a sample holder made of BN. This furnace can be operated with reducing atmospheres, vacuum or inert gases. It achieves a maximum temperature of 2000°C. Temperature is measured by a removable Pt30Rh–Pt6Rh (type B) thermocouple in an Al_2O_3 tube below 1400°C and by a two colour pyrometer monitoring the sample surface above 1000°C. The maximal heating rate is 50 K min^{-1} and the maximal cooling rate above 1000°C is 40 K min^{-1}. The other furnace uses $MoSi_2$ heating elements, an insulation made of alumina fibres and an Al_2O_3 sample holder. It is used for oxidizing atmospheres or inert gases and achieves a maximum temperature of 1650°C. Temperature is measured by a type B thermocouple, that is located about 10 mm beside the sample. Maximal heating rate is 5 K min^{-1} with this furnace and the maximal cooling rate above 1000°C amounts 20 K min^{-1}. Temperature gradients measured by a movable thermocouple in the central part of the chamber of the

furnaces are below 10 K cm^{-1} above 1000°C. Two of the three measuring sites are equipped with the graphite and $MoSi_2$ sintering furnace described above. The third one is used for measuring thermal diffusivities at room temperature.

Usually, Nd–YAG lasers with a wavelength of 1.06 μm are used with laser-flash measurements. Since many ceramic samples are transparent at that wavelength, special opaque coatings have to be used to deposit the laser pulse energy in the sample surface. Such coatings have many disadvantages (see below). Therefore, a pulsed CO_2-laser with a pulse energy variable among 30 and 80 J, a pulse time of 10–20 μs and a maximal repetition rate of 0.1 Hz is used with all three measuring sites for the measurements of thermal material properties. The wavelength of the CO_2-laser is 10.6 μm. The laser beam is directed into each of the independent measuring sites by movable Cu mirrors (Figs 1 and 3). A careful electromagnetic shielding of the laser is important to prevent disturbance of the measurements. Highly reflecting samples need the maximal pulse energy of the laser to give a sufficient increase of sample temperature for the laser-flash measurements. For other samples a much lower pulse energy is needed and pulse energy of the laser is reduced by placing metallic screens in the beam path.

The beam path for the thermal measurements is shown in Fig. 3. By adjusting the beam concentrator in the vertical direction, the diameter of the beam spot at the sample position can be changed. Usually disk shaped samples with a diameter of about 11 mm and a thickness of 1 mm are used. The front side of the samples is completely irradiated by the laser pulse. The energy of the primary laser pulse is monitored by an IR-detector. For that, a small fraction at the edge of the laser beam is lead by a metallic tube (inner width 2.0 mm) to the IR detector. The measurement of the intensity of the primary laser pulse is needed for the deter-

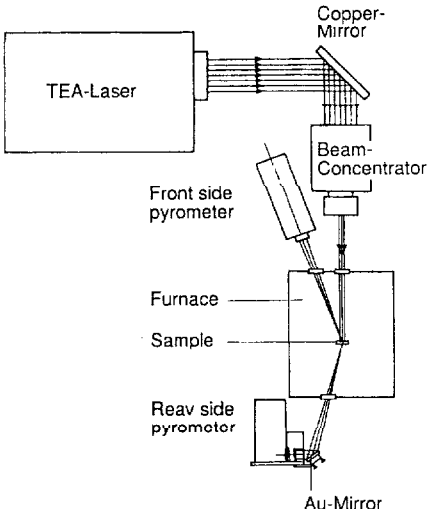

Fig. 3 Sketch of the optical beam path for the thermal measurements

mination of heat capacity. Two pyrometers monitor the front and the rear side of the sample. The pyrometer beam paths are in an angle of 15° and 165° from the centre to the vertical axis of the furnace. The wavelength range of the pyrometers can be changed by filters. The pyrometer at the rear side of the sample uses a filter with a range of 7.5 to 9.5 μm for laser-flash measurements. The same range is used by the pyrometer at the front side of the sample to monitor the temperature after the short heating by the laser pulse at the sample surface. The filter at the rear side pyrometer can be automatically exchanged by a 3 to 5 μm filter, which is used for the measurement of radiative transport in ceramic samples. The filter at the front side pyrometer can be exchanged automatically by a 10 to 11 μm filter that is used for the measurement of the diffuse reflected laser light from the primary beam. HgCdTe detectors are used in the pyrometers and the IR-detector for the laser beam. They are cooled by liquid nitrogen. The Dewar vessel has a hold time of 72 h. The diameter of the active detector area is 0.5 mm. The peak wavelength is 11 μm and the cut-off wavelength is 12.5 μm. The detectivity D^* has a value of about $5 \cdot 10^{10}$ cm $Hz^{1/2}$ W^{-1} and the responsivity is about 4.5 W at the peak wavelength. The electrical bandwidth of the detection system is 100 MHz. The temperature signal is amplified in two stages: in the detector amplifier, which is located near the pyrometer in order to reduce noise sensibility, and in an amplifier, which is located in the high speed data acquisition system in an industrial PC. The amplifications for the detector amplifier for the front side pyrometers are between 130 and 490 and for the rear side pyrometers between 1000 and 4500, depending on the detector's sensitivity and on the optical paths of the three measuring sites. The maximum amplification of the high speed data acquisition system is 50. The fastest sampling time is 200 ns per channel. The laser intensity IR-detector has an amplification factor of 50. All the amplifiers used are direct current amplifiers. For a typical temperature rise of 1 K in the sample, the signal noise ratio of the pyrometers at a sampling time of 10 μs is about 1.4, depending on the furnace temperature. By reduction of the sampling rate the signal noise ratio is enhanced. Usually a sampling rate is chosen, that is about 5 times higher than the inverse rise time. The signal noise ratio can be estimated from the equation:

$$S/N = (S/N)_{max} \, (s_{max}/s)^{1/2}, \tag{1}$$

where S/N and $(S/N)_{max}$ are the signal to noise ratios at sampling rate s and sampling rate s_{max}, respectively.

Each of the two furnaces is provided with one front side and one rear side pyrometer and a primary beam detector. Additionally it has a non-contact optical dilatometer, which uses the two opposing horizontal windows of the furnace. Figure 4 shows a sketch of the optical dilatometer. The components of the optical dilatometer are a 50 W halogen lamp with a condenser as a source of a parallel light beam, a telecentric objective (true telecentric working distance 5" to 15")

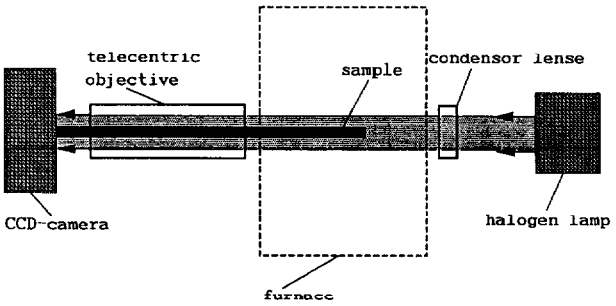

Fig. 4 Sketch of the optical dilatometer

and a 768×512 pixel CCD camera. The measurement area is 12.0×9.5 mm^2 giving a pixel resolution of about 20 μm. The tolerance of length measurements is improved by averaging within a measuring window. The measuring tolerance, for example, is about 10 μm for a window width of 0.2 mm. When the thermal radiation from the sample is bright, enough the halogen lamp is automatically switched off and the silhouette of the sample is measured in the inverse contrast. Sample radiation is usually strong enough at about 1500 to 1800°C. If the temperature in the furnace is rather high, the sample holder moves due to heat expansion with respect to the measurement area of the dilatometer. The software detects such a change and compensates for it. By this procedure, the windows stay at the same locations on the sample (Fig. 5).

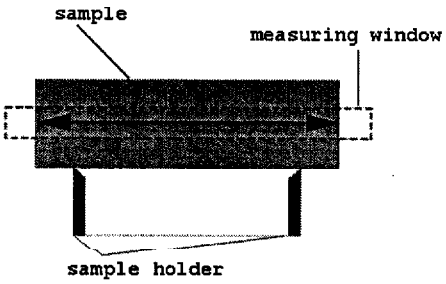

Fig. 5 Cross section of the disk shaped sample on the CCD camera of the optical dilatometer

The third measuring site (Fig. 1) is specially designed for accurate measurements of thermal diffusivity at room temperature. An aperture angle of 9° is used for the optical pyrometer at this site. Additionally, at this measuring site an angle resolved measurement of diffuse reflected laser light from the sample surface is possible. A pyrometer that is mounted to a goniometer is used for that task and is movable between angles of 15° and 60° to the laser beam.

Data collection and control of the TOM System is done by microcontrollers and personal computers which are connected in a network. As only one laser is

available in this system, an assignment management must be used for simultaneously operating the TOM system with 2 or 3 sites, because for every measurement a laser flash is necessary. This management is carried out by the main computer. The main computer is equipped with three high speed data acquisition boards. In every measurement 3 data channels are recorded simultaneously: front side and rear side pyrometers and the IR-detector for the primary laser pulse. The channels are allocated to each measuring site by a multiplexer. The sequence of operation for a typical sintering cycle is as follows:

1. The temperature profile and the sequence of measurements are determined in an ASCII control file for each measuring site. The input is, e.g., heating rates, temperatures of isothermal sequences, number, time and kind of measurements.
2. The subsequent temperatures determined in the control file are sent to the furnace electronics which raises the temperature to these values.
3. When the temperature is constant, an electronic compensation for a zero temperature rise is performed with the data acquisition boards, before laser flash measurements are started.

Data evaluation

During sintering, measuring data are accumulated from the two pyrometers, from the primary beam detector and from the dilatometer about every 2 to 5 min. To allow a feedback control of the furnace temperature by the measured results, a fast automatic on-line evaluation of the measured data has been developed. Additionally, the complete data set is stored on magnetic disk after each measuring cycle and can be used for a detailed data evaluation later on. The diameter of the sample is determined by averaging the horizontal dimension of the silhouette of the disk shaped sample that is within the measuring window of the dilatometer (Fig. 5). Shrinkage is calculated by dividing the difference of the initial sample diameter and the actual sample diameter by the initial sample diameter. The initial sample diameter is measured in the same arrangement before heating is started. By assuming isotropic shrinkage of the sample, sample thickness is calculated from the decrease of sample diameter. The initial sample thickness is measured by a micrometry screw. This indirect determination of sample thickness gives a better accuracy than the direct determination since sample thickness is usually 1 to 3 mm and, therefore, much smaller than the diameter. Moreover, a slight tilting of the sample or a deformation of the sample surface, which can occur during sintering, affects the sample thickness measurement, but not the determination of the diameter by the projection method used in the TOM system. An accurate determination of sample thickness is important, since thermal diffusivity depends on the square of sample thickness (Eq. 4). The two-dimensional measurement of the silhouette of the sample is useful for monitoring phenomena

other than sintering shrinkage. Three of these phemomena have already been investigated:

– The wetting behaviour of a liquid droplet on a flat solid substrate. Contact angle is determined by fitting the contour of the shadow of the droplet [19]. The wetting behaviour is important in liquid phase sintering.

– The sintering stresses in layered composite materials. If the substrate is thin enough, warping of the composite is observed (bimaterial dilatometry [20]).

– The occurrence of sintering cracks in components with complex shapes.

Figure 6a shows a sample, that has a wedge shaped groove at its top side and sticks to a non-sintering substrate at its bottom side at a temperature of 700°C. After the onset of sintering shrinkage, a crack is produced in the wedge, and the sample breaks to two pieces (Fig. 6b). The crack starts at the tip of the wedge, when sintering stresses become larger than the tensile strength of the sintering necks. Stress in the wedge tip is proportional to the cosine of half of the aperture angle. Therefore, by varying the shape of the wedge in the green compacts different stresses are produced during sintering.

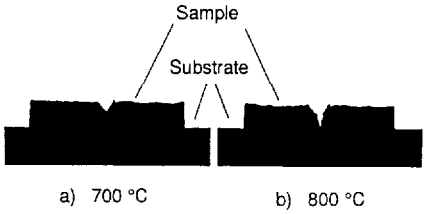

Fig. 6 In situ monitoring of sintering crack formation in one dimensional sintering by the TOM system: a) before and b) after crack formation at the top of the wedge shaped groove at the sample surface

For the determination of the specific heat capacity of the sample, the fraction of the pulse energy E_{abs}, which is absorbed by the sample, has to be determined. This is done indirectly from the energy E_0 of the primary beam and from the fraction E_{ref}, that is reflected by the sample. E_0 is measured by the primary beam detector. Figure 7 shows the measuring data from this detector. The peak integral I_0 is proportional to the pulse energy of the laser beam. For a fixed optical beam path the coefficient of proportionality can be calibrated by measuring the temperature rise ΔT in a completely absorbing sample of known heat capacity. E_{ref} has to be determined from the measuring data of the from side pyrometer (Fig. 8b), which supplies the peak integral I_{ref} analogous to the primary beam detector. From the small solid angle, that is covered by the front side detector, only a small fraction of the reflected energy is detected. By measuring the reflected energy for different angles, the calculation of E_{ref} from I_{ref} can, in principle, be performed. This measurement can be done at the third measuring site (see previous section). Since the spatial distribution of the reflected light depends on the microstructure of the surface, the sample has to be measured in the same state of

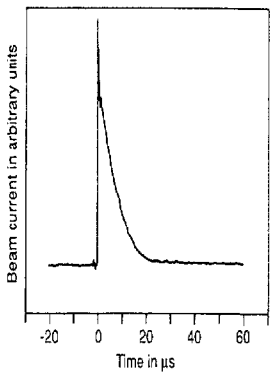

Fig. 7 Typical measuring signal of the IR-detector for the primary laser pulse

sintering as in the furnace. (Two other conditions are necessary for the transfer of room temperature measurements to sintering samples: the reflection coefficient has to be independent of temperature and the sample surface may not be altered by the laser beam.) The absorbed energy of the laser and its effect on rear side temperature, which is measured by the rear side pyrometer, gives a measure of heat capacity of the sample:

$$E_{abs} = E_o \quad E_{ref} = c_p m \Delta T. \tag{2}$$

where c_p is the specific heat capacity at constant pressure, m is the sample mass and ΔT is the temperature rise of the sample that is determined from Eq. (3).

Figure 9a shows typical measuring data of the rear side pyrometer. The temperature curve is described by the function [21]:

$$T(t) = 2\Delta T d \sum_{k=1}^{\infty} \beta_k \exp(-\alpha \beta_k^2 t) \frac{\beta_k \cos(\beta_k d) + l \sin(\beta_k d)}{(\beta_k^2 + l^2)d + 2l} \tag{3}$$

where β_k are the positive roots of $\tan(\beta_k d)=2l/(\beta_k^2-l^2)$, d is the sample thickness, α is thermal diffusivity, ΔT is the temperature rise in the adiabatic limit and l is a loss factor describing the heat loss at the front and rear side of the sample.

This function is fitted to the measuring data by a least square fitting algorithms running off-line on a personal computer. (A correction of the temperature rise, due to the finite pulse time of the laser, which is usually applied in laser-flash measurements [13], is not necessary with the TOM system because the pulse time of the CO_2 laser is very short.) Thermal diffusivity α, temperature rise ΔT, loss factor l and reduced χ^2 which is a measure of the reliability of the fit are the output of this computer program. For a fast on line evaluation of the thermal diffusivity only the time $t_{1/2}$ for the rise of temperature to half of its maximum

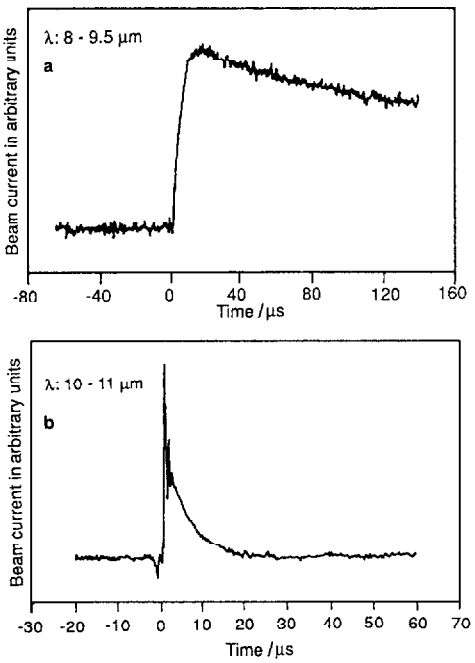

Fig. 8 Measuring signals of the pyrometer monitoring the front side of the sample (Al_2O_3 at 1600°C); wavelength region: a) 8 to 9.5 µm (temperature measurement) and b) 10 to 11 µm (measurement of reflected laser light)

value and the heat loss are determined [22]. From $t_{1/2}$ the thermal diffusivity is calculated according to the equation [6]:

$$\alpha = 1.38 \frac{d^2}{\pi^2 / t_{1/2}} \tag{4}$$

By changing the filter in the optical beam path of the rear side pyrometer to a region of shorter wavelengths many ceramic materials become semitransparent. For alumina, radiative transport mainly depends on scattering and not on absorption in a wavelength region between 3 and 5 µm [23, 24]. Therefore, the temperature rise at the front side of the sample is instantaneously detected by the rear side pyrometer by the heat radiation which is transmitted through the sample (Fig. 9b). The step height h is determined by a linear fit of a vertical line and two adjacent lines in the step region of the detector signal and calculating the distance of the intersections. The light transmission ratio r is calculated from the step height by normation with the total increase of intensity ΔI (Fig. 9b):

$$r = h/\Delta I. \tag{5}$$

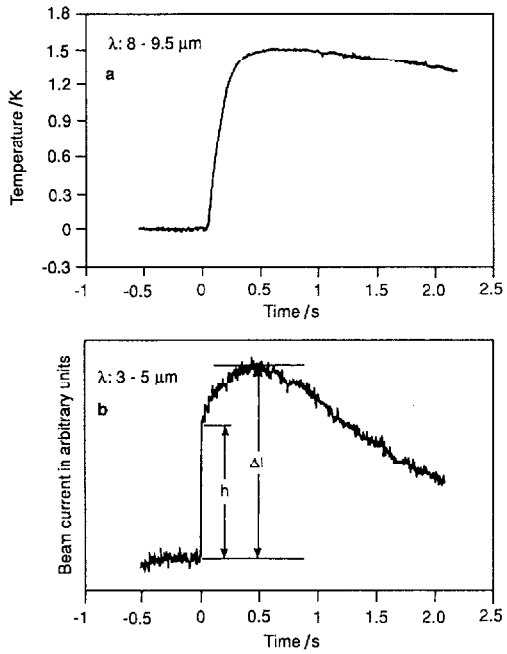

Fig. 9 Measuring signals of the pyrometer monitoring the rear side of the sample (Al_2O_3 at 1600°C); wavelength region: a) 8 to 9.5 µm (temperature measurement for laser-flash technique) and b) 3 to 5µm (measurement of heat radiation, symbols are explained in the text)

The front side temperature recorded by the front side pyrometer using the filter 7.5 to 9.5 µm is shown in Fig. 8a. The decreasing part of the curve is described by the equation [21]:

$$T(t) = 2\Delta T d \sum_{k=1}^{\infty} \exp(-\alpha\beta_k^2 t) \frac{\beta_k^2}{(\beta_k^2 + l^2)d + 2l} \tag{6}$$

where the meaning of the symbols is the same as in Eq. (3). In layered samples the decrease of front side temperature depends on the thermal resistance between the layers [25]. Since the thermal resistance depends on the adhesion between the layers, delamination phenomena can be studied in situ by monitoring of the front side temperature in the TOM system.

Thermal conductivity λ is calculated from density ρ, specific heat c_p and thermal diffusivity α by the simple equation [21]:

$$\lambda = \rho c_p \alpha. \tag{7}$$

Results and discussion

The reproducibility of the determination of sample diameters with the optical dilatometer is 10 μm or 0.1% (standard deviation). The same value was determined for its accuracy by measuring standard gauges. The resolution of push rod dilatometers that are usually applied in sintering studies, is much better than 1 μm. (Interferometric length measurements allow an even better length resolution, but they are very sensitive to disturbances like density gradients in the furnace atmosphere.) A resolution below 1 μm rarely can be used in sintering experiments with powder compacts, because a much larger error is produced by differential sintering, due to density gradients in the green compacts. (A radial density gradient of 1% of fractional density in a cylindrical green compact of 1 cm length produces a differential sintering effect as large as 30 μm at the faces.) Since density gradients in green compacts are inevitable, not so much the resolution of the dilatometer system is important, but rather the reproducibility with sintering samples. This reproducibility depends on the sample volume, that really contributes to the length measurements. Differential sintering leads to a deformation of the sample faces if there are radial density gradients in the green compact, which is likely in cylindrical cold isostatically pressed samples. With push rod dilatometry only the most prominent parts of the faces determine the measured length of the sample which significantly reduces measured volume and reproducibility. By measuring the projection of the convex lateral area of disk shaped samples with the TOM system, this problem should not arise. However, reproducibility might be worse for samples with strong axial density gradients, since sample height is only 1 to 3 mm. For cylindrical alumina compacts that were prepared by cold isostatic pressing and cut to slices afterwards, the measured reproducibility was better than 0.3% during the complete sintering cycle with the TOM system. Total linear shrinkage during sintering is usually about 15%. Considering the reproducibility of the optical dilatometer for different samples of 0.3% about 50 different status of the sample can be distinguished. If only one sample is examined, the reproducibility of 0.1% can be used and about 150 states can be distinguished. To compare the potential of different in situ measuring methods a resolving power is defined, which is just the number of different states that can be distinguished in a usual sintering experiment by the respective method. Therefore, for the non-contact dilatometer the sample to sample resolving power is about 50 and the one sample resolving power is 150.

The determination of heat capacity be equation 2 is tedious, since the energy of the laser pulse E_o and the reflected fraction E_{ref} have to be determined by a number of calibrations. To register material changes during sintering, relative measures are sufficient and calibration work can be reduced. The potential of the method can be estimated by determining the reproducibility of the measurement of the two peak integrals I_o and I_{ref} and the temperature rise ΔT. For a sintered alu-

mina sample at temperatures between 1000 and 1600°C the reproducibilities of I_o, I_{ref} and ΔT have been determined:

$$\sigma(I_o)/I_o = 1\% , \quad \sigma(I_{ref})/I_{ref} = 4\% , \quad \text{and} \quad \sigma(\Delta T)/\Delta T = 2\%.$$

Therefrom, it is estimated that the reproducibility in measurements of heat capacity is about 4%. Changes of the heat capacity are mainly caused during a sintering process by the temperature changes. The residual change that is caused by phase transformations is usually below a few % [26]. Therefore, the resolving power of heat capacity measurement by this method is very low and the method will only be useful for a rough distinction of states in special cases. DSC devices achieve a reproducibility of about 1% and can register the heat of reactions additionally [27]. Specific heat measurements will have to be improved before the advantage of simultaneous measurements with the TOM system can be fully used. Nevertheless, the ratio I_{ref}/I_o showing significant changes during sintering can be used to detect the development of surface structure.

Vitreous, ceramic and metallic materials cover a broad range of thermal diffusivities from 0.3 to 300 $mm^2 s^{-1}$ [28]. Therefore, for dense samples at room temperature the rise time in laser-flash measurements varies among 5 ms and 0.5 s for a typical sample thickness of 1 mm according to Eq. (4). (For green compacts the thermal diffusivity is lower by about 1 or 2 orders of magnitude than for dense samples [29] and there is also a strong decrease of thermal diffusivity with increasing temperature [30]). The energy, that can be put into the sample by the laser pulse is limited, since non-linear effects falsify the measurements, if the temperature rise is above some K [7]. The sintering process may also be disturbed by a higher energy input. Therefore, the pulse energy of the laser was adjusted to give a temperature rise of about 2 K in the thermal diffusivity measurements. Due to equation 1 the signal noise ratio for the smallest rise times of 5 ms is about 30. For large rise times not the signal noise ratio but non-linear temperature shifts of the furnace limit the reproducibility of the laser-flash measurements. The reproducibility of the thermal diffusivity measurements with the TOM system was about 2% in a temperature range between room temperature and 2000°C for different materials. For different alumina green compacts that were measured in subsequent sintering runs, the reproducibility of thermal diffusivity was better than 5%. The accuracy was tested by a pure Fe sample. The thermal diffusivity measured by TOM at room temperature was 23.5 $mm^2 s^{-1}$ which is in good agreement to literature data (α=22.2 $mm^2 s^{-1}$ [31]). For dense polycrystalline α-alumina the measured thermal diffusivity at room temperature is 11.2 $mm^2 s^{-1}$ compared to 9.1 $mm^2 s^{-1}$ in the literature [32]. Figure 10 shows the thermal diffusivity and density of an alumina compact, that was sintered with a heating rate of 10 K min^{-1}. Thermal diffusivity increases by a factor of 10 from 0.1 $mm^2 s^{-1}$ at low temperature to 1.1 $mm^2 s^{-1}$ at 1650°C. Considering the reproducibility of 5% for different samples, a sample to sample resolving power of 50

is determined. Analogous from the reproducibility of 2%, a resolving power of 120 is calculated for measurements of one sample.

Due to their very high resolving power, thermal diffusivity measurements have a large potential in sintering studies. However, to learn about microstructure of the samples from in situ measurements of thermal diffusivity, the mechanisms have to be known, which influence heat transport at high temperatures. Thermal diffusivity decreases with increasing temperature by a reduction of free phonon path length due to an increasing contribution of phonon-phonon scattering [30]. Care has to be taken in comparing high temperature results of different laboratories since measured results depend somewhat on the experimental arrangement. Besides the heat conduction, heat radiation also contributes to the transport of thermal energy. Its importance depends on the way the heat is transferred to and measured at the surfaces of the sample [23]. The experimental arrangement, chosen in the TOM system for the laser-flash measurements largely suppresses radiative transport, since absorptive coatings that usually have a high emissivity at the front side of the sample and absorb all radiation at its rear side are omitted. Nevertheless radiative transport contributes to the total heat transport at 850°C in Fig. 10 as much as 10% with the TOM system [23]. For porous compacts there is also a contribution of heat conduction in the gaseous pore phase to the total heat transport besides the heat conduction in the solid phase. Therefore, the compact has to be treated as a two phase system, where the conductivity of one of the two phases is lower than the other by two or three orders of magnitude. The conductivity depends strongly on the microstructure of the compact. In the initial phase of sintering, the constriction resistance at the particle contacts determines the conductivity of the sample [33]. Thermal conductivity is proportional to the neck radius under the condition of small sintering necks [34]. Therefore, in the first stage of sintering the formation of sintering necks can

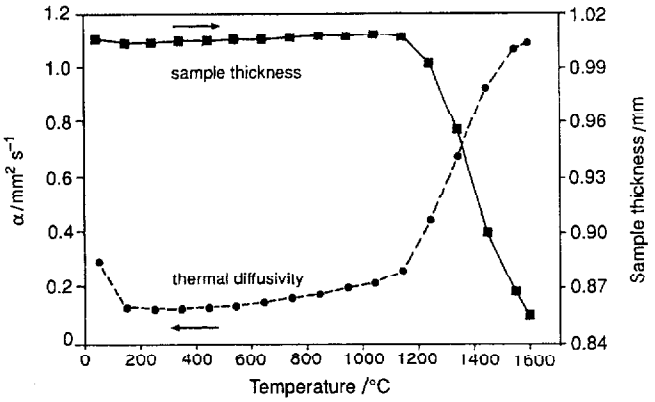

Fig. 10 Simultaneous measurement of thermal diffusivity α and shrinkage with the TOM system during sintering of a cold isostatically pressed Al_2O_3 green compact (Alcoa A 16 SG without any additives)

be observed by thermal diffusivity. By contrast, dilatometry often is not useful for this purpose because sintering necks can form without any shrinkage by transport of atoms from the particle surfaces to the neck region [35]. A detailed description of the in situ measurement of sintering neck growth by thermal diffusivity is given in another paper. In the intermediate stage of sintering there is a mutual penetration of pore phase and solid phase and the increase of thermal conductivity is roughly proportional to the increase of density [36]. The same holds true for the final stage of sintering, when the pores are isolated. Therefore, in the intermediate and final stages of sintering thermal diffusivity will give similar information on microstructure as shrinkage measurement. Since the thermal diffusivity strongly decreases by the formation of cracks [36], microcrack formation can be detected by a deviation from the simple linear relation between shrinkage and conductivity. Considering liquid phase sintering, a strong influence of the formation of the liquid phase on thermal diffusivity has been observed. A wetting liquid flows to the particle contacts, which strongly influences their thermal resistance [33]. The formation of solid particle contacts can also be detected in liquid phase sintering. Since the solid conductivity depends on the free phonon path length, dislocations, impurities or other lattice defects in crystalline samples which reduce this wavelength may be investigated by measuring the temperature dependence of thermal conductivity [37].

Conclusions

The requirements considering the transferability of TOM results to other sintering furnaces demand compromises in the design of the TOM system. To achieve a homogeneous temperature in the furnace, only a very small solid angle is available for the detectors. To avoid special coatings of the sample during the laser-flash measurements, an expensive CO_2 laser has to be used and the pyrometers have to be run in the far infrared range. Nevertheless, completely non-contact measurement of thermal properties and the simultaneous non-contact measurement of shrinkage has been achieved. The sample volume is usually about 0.1 cm^3. By using the front side pyrometer for the thermal diffusivity measurement, it can be enlarged to a few cm^3. Compared to conventional push rod dilatometers, the resolution of the optical dilatometer of the TOM system is inferior but in sintering studies very high resolutions cannot be used anyway and the two dimensional image of the samples given by the optical dilatometer allows investigations of additional phenomena. The resolving power of specific heat measurements with the TOM system is too low to detect small changes which may occur during sintering. Unlike specific heat, a very high resolving power was achieved for the thermal diffusivity measurements. Therefrom, new insight in sintering processes can be expected. Especially changes in the microstructure like the formation of sintering necks, microcrack formation and liquid phases

have a strong impact on thermal diffusivity. Such phenomena can now be investigated in situ with the TOM system. Moreover, the design of the TOM system allows the addition of optical measuring methods, which have a high resolving power in the final stage of sintering.

For the optimization of time-temperature-atmosphere cycles of sintering processes a significant improvement of efficiency can be expected from the TOM system. Since an interruption of the heat treatment can be avoided by the in situ measurements in many cases, optimization can be carefully directed to more demanding goals. Also, an extension of the RCS approach can be used since other properties other than sintering shrinkage are available for temperature control.

* * *

The authors are very indebted to M. Güther (company Hoechst) for the stimulation of this development and valuable discussion. They thank O. Hahn, M. Magnor and J. Fricke (University of Würzburg) for valuable discussion. We are also grateful to numerous people who took part in the assembly of the system.

References

1 F. Thümmler, Wissenschaft und Praxis, 5 (1989) 261.
2 S. Winkler, P. Davies and J. Janoschek, J. Thermal Anal., 40 (1993) 999.
3 H. Palmour, Sci. Sintering, 7 (1989) 367.
4 P. Komarenko and R. W. Messler, Int. J. Powder Metall., 30 (1994) 67.
5 M. L. Lyamshev, J. Stanullo and G. Busse, Materialprüfung, 37 (1995) 1.
6 W. J. Parker et al., J. Appl. Phys., 32 (1961) 1679.
7 R. Enck and R. D. Harris, Mat. Res. Soc. Symp. Proc., 167 (1990) 235.
8 M. Güther and H.-J. Sölter, Apparat und Verfahren zur Tempareturleitfähigkeitsmessung, Patent DE 4131040, 1995.
9 D. P. H. Hasselmann, R. Syed and T.-Y. Tien, J. Mat. Science, 20 (1985) 2549.
10 D. P. H. Hasselmann, L. J. Johnson, L. D. Bentsen, R. Syed. H. L. Lee and M. V. Swain, Am. Ceram Soc. Bull., 66 (1987) 799.
11 M. J. Wheeler, Brit. J. Appl. Phys., 16 (1965) 365.
12 A. G. Shashkov, S. Yu Yanovskii and T. N. Abramenko, High. Temp.-High Press., 16 (1984) 93.
13 H.-J. Sölter, Das Laserpulsverfahren zur simultanen Bestimmung der Temperatur- und Wärmeleitfähigkeit von Zweischichtsystemen: Vergleich von Auswertungsformalismen und Untersuchungen an plasmagespritzten Schichten, Dissertation, Universität Stuttgart 1990. IKE–5–231, ISSN 0173–6892.
14 R. A. Nyquist and R. O. Kagel, Infrared Spectra of Inorganic Compounds, Academic Press, San Diego 1971.
15 W. W. Chen and B. Dunn, J. Am. Ceram. Soc., 76 (1993) 2086.
16 S. Meyer, Apparatur zur Messung von kohärenter Laserlichtstreuung, Diplomarbeit, Fachhochschule Gießen-Friedberg and Fraunhofer-Institut für Silicatforschung, Würzburg 1996.
17 M. Pfeffer, Programmierbarer Gasmischer, Diplomarbeit, Fachhoshschule Gießen-Friedberg and Fraunhofer-Institut für Silicatforschung, Würzburg 1996.
18 G. Neubert, Aufbau eines pneumatischen Positioniersystems mit Mikrocontroller-Steuerung, Diplomarbeit, Fachhochschule Würzburg-Schweinfurt and Fraunhofer-Institut für Silicatforschung, Würzburg 1994.

19 M. E. R. Shanahan, J. Chem. Soc., Faraday Trans. 1, 80 (1984) 37.
20 M. P. Borom and C. A. Johnson, Surf. Coat. Technol., 54–55 (1992) 45.
21 H. S. Carlslaw and J. C. Jaeger, The conduction of heat in solids, Oxford Univ. Press, Oxford 1976, p. 118.
22 R. C. Heckman, J. Appl. Phys., 44 (1973) 1455.
23 O. Hahn, F. Raether, M. C. Arduini-Schuster and J. Fricke, Int. J. Heat and Mass transfer, (1995).
24 N. Grimm, G. E. Scott and J. D. Sibold, Ceramic Bull., 50 (1971) 962.
25 A. C. Tam and H. Sontag, Applied Phys. Letters, 49 (1986) 1761.
26 I. Barin, Thermochemical Data of Pure Substances, VCH Verlagsgesellschaft, Weinheim 1989.
27 W. F. Hemminger and H. K. Cammenga, Methoden der termischen Analyse, Springer, Berlin 1989.
28 U. Grigull and H. Sandner, Wärmeleitung, Springer-Verlag, Berlin 1990.
29 F. Raether and G. Müller, New in situ measuring methods for the optimization of sintering processes, Proceedings IV ECerS-Tagung, Riccione, Italy (1995) 103–112.
30 G. A. Slack, Nonmetallic crystals with high thermal conductivity, J. Phys. Chem. Solids, 34 (1973) 321–335.
31 A. J. Walter, R. M. Dell and P. C. Burgess, Rev. Int. Hautes Temp., Refract. 7 (1970) 271.
32 W. H. Gitzen, Alumina as a Ceramic material, American Ceramic Society Inc., Columbus/Ohio 1970, p. 66.
33 O. Hahn, F. Raether and J. Fricke, Heat transfer at particle contacts in the presence of gases and/or liquid secondary phases, submitted to Int. J. of Thermophysics (1996).
34 Y. Ogniewicz and M. M. Yovanovich, Effective conductivity of regularly packed spheres: basic cell model with constrictions. Prog. Astronaut. Aeronaut., 60 (1978) 209.
35 G. Ondracek, J. of Materials Technology, 5 (1974) 416.
36 D. Uskokovic, The kinetics of Contact Formation during sintering by diffusion mechanisms, Science of Sintering, 9(3) (1977) 265.
37 G. A. Slack, R. A. Tanzilli, R. O. Pohl and J. W. Vandersande: The intrinsic thermal conductivity of AIN, J. Phys. Chem. Solids, 48 (1987) 641.